Communications

Crystallographic Analysis of Primary Visual Photochemistry**

Hitoshi Nakamichi and Tetsuji Okada

Photochemical *cis–trans* isomerization of the retinylidene chromophore is the mechanism of the primary visual process in the eye. 11-*cis*-Retinal is covalently linked not only to the dim-light photoreceptor protein rhodopsin but also to each of the three color pigments in humans. All of these proteins belong to the superfamily of G protein coupled receptors (GPCRs). To achieve extreme sensitivity for photon detection, the photoisomerization reaction to the all-*trans* form in these pigments has to be strictly designed for efficient formation of the active form of the protein moiety, which catalyzes guanosine diphosphate to triphosphate (GDP–GTP) exchange in the α-subunit of the G protein. To understand the molecular mechanism of this primary photochemistry, detailed structural analysis is required. Recent advances in X-ray crystallographic studies of rhodopsin[1–3] have opened a way to investigate the photoreaction with subatomic resolution.

The first intermediate that can be trapped following light absorption by rhodopsin is bathorhodopsin (Figure 1 a). Formation of bathorhodopsin occurs on an ultrafast timescale of a few hundred femtoseconds at room temperature.[4] It exhibits a high quantum yield of 0.67[5] and stores about two-thirds of the photon energy (36 kcal

mol^{-1}),[6] which is used to drive the formation of subsequent intermediates. Spectroscopic studies at low temperature or with time resolution yielded indirect structural data for this photochemical intermediate. Resonance Raman spectra of trapped bathorhodopsin indicated a strongly distorted chromophore in the region where the isomerization has taken place;[7] this distortion was recently substantiated and quan-
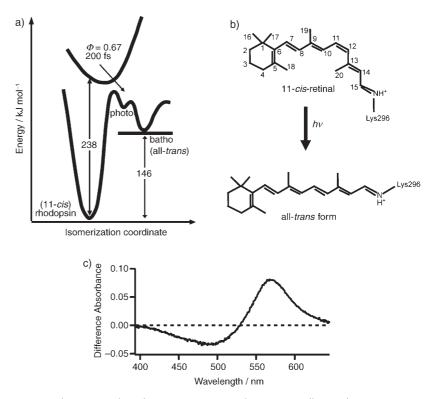

Figure 1. The primary photochemistry in vision involves 11-*cis* to all-*trans* photoisomerization of retinal. a) Schematic drawing of energy changes during the photoisomerization reaction. The photochemical precursor of bathorhodopsin is not detectable under cryogenic conditions. b) Chemical structure of the two isomeric forms of retinal before and after photoisomerization. The numbering scheme of carbon atoms is shown for 11-*cis*-retinal. c) Spectral changes observed upon conversion from rhodopsin to bathorhodopsin in a three-dimensional crystal at 105 K. A difference spectrum before and after illumination with 488 nm light is shown.

[*] H. Nakamichi, Dr. T. Okada
Biological Information Research Center
National Institute of Advanced Industrial Science and Technology
2-41-6 Aomi, Koto-ku, Tokyo 135-0064 (Japan)
Fax: (+81) 3-3529-5379
E-mail: t-okada@aist.go.jp
and
Core Research for Evolution Science and Technology (CREST)
Japan Science and Technology Agency (Japan)

Supporting information for this article is available on the WWW under http://www.angewandte.org or from the author.

tified to some extent.[8] Photoaffinity labeling studies of the bathorhodopsin intermediate indicated that the "loose" end of the chromophore, that is, the β-ionone ring, does not change its position relative to the dark state,[9] confirming the notion that the perturbation caused by the photoreaction is initially localized on a relatively small part of the chromophore. This view is supported by recent solid-state NMR spectroscopic observations of the methyl groups of the β-ionone ring which show that the ring is retained through strong selective interactions within the binding site into the activated state.[10] Also, magic-angle spinning solid-state NMR spectra of isotopically labeled bathorhodopsin revealed only minor differences in chemical shifts compared to rhodopsin, indicating that the protein environment of the chromophore, in particular the interaction with the counterion Glu113, does not change significantly.[11]

4270

WILEY InterScience® DISCOVER SOMETHING GREAT

© 2006 Wiley-VCH Verlag GmbH & Co. KGaA, Weinheim

Angew. Chem. Int. Ed. **2006**, *45*, 4270–4273

Herein, we report the first structural view of bathorhodopsin examined by X-ray crystallography of illuminated rhodopsin crystals under cryogenic conditions. Structural changes in the protein environment induced by the conformational change of the chromophore suggest possible pathways towards the activated state of rhodopsin.

To study the structural differences between rhodopsin and bathorhodopsin, X-ray diffraction data were collected from frozen crystals with and without illumination. Crystals exposed to light with a wavelength of 488 nm at 95 K produced a red-shifted absorption spectrum (Figure 1c), which was similar to that of bathorhodopsin in solution. Under almost identical conditions to this offline spectroscopy, crystals were illuminated during collection of the diffraction data. The building of the model of bathorhodopsin was guided by difference electron densities, which were calculated with two data sets obtained before and after illuminating a crystal that reveals only a negligible amount of twinning (data set 2, see Supporting Information). Most of the large peaks were found only in the limited regions around the retinal unit (Figure 2a) and consistently in the two molecules in the asymmetric unit. The residues associated with the prominent peaks (3.5 σ) are Cys110, Glu113, Thr118, Glu122, Cys167, Cys187, Met207, Phe212, Trp265, Tyr268, and Lys296 (Figure 2b,c). A control difference map calculated with two data sets collected sequentially from a crystal without illumination
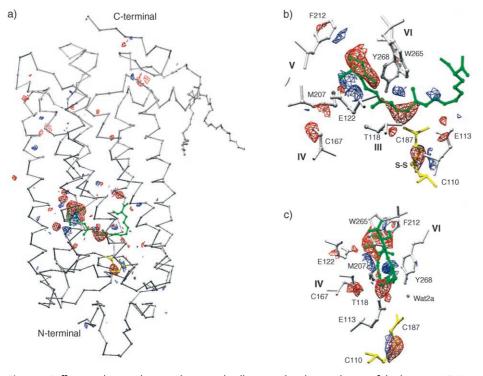
showed no significant signals, indicating that the effect of radiation damage to the crystal was negligible (data not shown).

The pattern of difference densities corresponding to retinal was unexpected: a pair of strong positive and negative densities appeared at the β-ionone ring and around the C11=C12 bond (Figure 2b,c). This finding is not consistent with a simple one-bond flip for the photoisomerization process. We confirmed these differences between rhodopsin and bathorhodopsin in a number of data sets, two of which are shown in the Supporting Information. The structure refinement of bathorhodopsin was continued with one of these data sets, data set 1. Although the resolution of our data is not very high and is comparable with that of the lowest resolution model of the primary K state of bacteriorhodopsin, the clear difference electron densities calculated from the data with negligible twinning provide strong evidence for the magnitude and direction of the atomic displacement.[12]

Difference electron-density maps were also used to determine the ranges of amino acid residues that should be included in the refinement. We chose Asp83–Thr94, Cys110–Glu122, Glu181–Gly188, Tyr206–Phe212, Trp265–Gly270, and Pro291–Ala299 as the region that was large enough to cover all of the possible differences between rhodopsin and bathorhodopsin. Then, by taking only the reproducible and substantial structural differences, 11 residues as noted above were selected in the final alternate conformation refinement with an optimized ratio of rhodopsin and bathorhodopsin (see Experimental Section).

The structural change of the retinal polyene chain from rhodopsin to bathorhodopsin is small at the carbon atoms C9, which has a methyl group attached, and C13 (Figure 3a,b). The C11=C12 bond is displaced towards the cytoplasmic side, in the vicinity of Trp265 in transmembrane helix (TMH)-VI, while the chain from C7 to C9 and the β-ionone ring move downward in a seesaw-like fashion with C9 at the center (Figure 3c). The dihedral angle around the C11=C12 bond changes from about −40° to −155° upon isomerization, with a substantial rotation of the methyl group at C13 in the same direction as the pre-twist in rhodopsin. Overall, the polyene chain of retinal is quite distorted, with all dihedral angles around the double bonds lying in the range from −150° to −170°. The largest twist among the

Figure 2. Difference electron densities between the illuminated and ground state of rhodopsin at 95 K (see text for details). a) $F_{light} - F_{dark}$ map calculated to 2.7 Å resolution is superimposed on the α-carbon trace of the structure of rhodopsin. The map is contoured to 3.5 σ (red, negative; blue, positive) for one of the two molecules in an asymmetric unit. The chromophore (11-*cis*-retinal + Lys296) and a disulfide bond between Cys110 and Cys187 are colored green and yellow, respectively. b) An expanded view of the map shown in part (a) highlighting the region around retinal and the residues associated with difference electron densities. c) A different view of the same region as in part (b) rotated approximately 90° around a vertical axis. The helices are numbered III–VI.
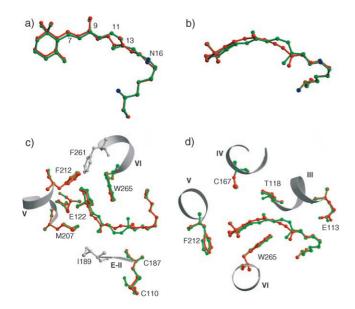
Figure 3. Structural changes from rhodopsin (green) to bathorhodopsin (red). a) A view of retinal and Lys296 linked through a protonated Schiff base from the direction similar to Figure 1b. Nitrogen atoms are shown in blue (see Supporting Information for a stereochemical view of this figure). b) A different view of the chromophore rotated approximately 90° around a horizontal axis, highlighting the curvature along the polyene chain in bathorhodopsin. c) Part of the retinal-binding pocket and the structural changes viewed from the direction similar to that used in Figure 2a,b. d) A different view of the retinal-binding site.

single bonds is found at the C12–C13 position. This first crystallographic model of the retinal in bathorhodopsin has not been predicted by previous models such as the hula-twist mechanism (see Reference [13] for more details).

The position of the Schiff base does not change significantly, whereas a small displacement of the side chain of Glu113 is consistently found in all the data sets containing bathorhodopsin (Figure 3d). As a result, the distance between the protonated Schiff base (the position of nitrogen atom N16) and the counterion (average of OE1 and OE2 of E113) increases slightly from 3.6 Å (chain A) and 3.4 Å (chain B) in rhodopsin to 3.9 Å (chain A) and 3.7 Å (chain B) in bathorhodopsin. This constant difference of 0.3 Å between the two states may not be large compared with the differences of 0.2 Å between the two molecules in the asymmetric unit for both rhodopsin and bathorhodopsin. Whether such an increase in the distance between the Schiff base and counterion is consistent with theoretical considerations is discussed in Reference [13]. This parameter also affects the estimation of energy storage in bathorhodopsin.

A small but substantial displacement of the polyene chain in retinal from C8 to C10 causes perturbation at Thr118 in TMH-III, which in turn moves outward from the core of protein. Another interesting feature in TMH-III is the difference electron density around the S—S bond that connects Cys110 and Cys187 in the second extracellular loop (E-II). The carbonyl oxygen atom of Cys187 is one of the atoms that is in close contact with retinal. Its distance to C12 of the retinal chain is about 3 Å in rhodopsin. As a result of

the configurational change in bathorhodopsin, the restraint keeping the positions of these two atoms disappears. As a consequence, the carbonyl oxygen atom of Cys187 relaxes, with a concomitant dislocation of the S—S bond (Figure 3c). We speculate that all these features associated with TMH-III and E-II indicate the initial trigger evoked in rhodopsin for a further thermal activation process, which will be discussed later.

A pair of clear positive and negative difference densities appears reproducibly at the side chain of Phe212 in TMH-V, which forms part of the binding pocket for the β-ionone ring (Figure 2b). Owing to the translational dislocation of the cyclohexene ring upon isomerization, the aromatic ring of Phe212 moves inward to fill part of the space that the chromophore occupied in rhodopsin (Figure 3d). Interestingly, the position of that residue is also near to the agonist-binding site in adrenergic receptors[14,15] that may share a common activation mechanism with rhodopsin. Similarly, the side chain of Trp265 in TMH-VI rotates slightly to partially balance the loss of interaction with the β-ionone ring. Because most rhodopsin-like GPCRs share tryptophan at this position, our model of bathorhodopsin suggests a general mechanism of activation for this class of GPCRs.

Our findings from crystallography studies provide valuable insights into the molecular mechanisms by which the primary process of vision is mediated, and we propose the following thermal activation process. We postulate that photon absorption causes isomerization of retinal in a seesaw-like mechanism, which initiates a small displacement of the β-ionone ring (Figure 3c). The direction of this movement is defined by the binding pocket that has a space at the extracellular side of the ring. The only residues that are within 4.5 Å from atoms C16, C17, and C7 are Ile189 in E-II and Met207 in TMH-V, whereas the cytoplasmic side (C3, C4, and C18) is surrounded by the peptide from Gly121 to Glu122, the side chains of Phe212, Phe261, and Trp265. Similarly, atoms C11 and C12 do not have any residues within 5 Å at the cytoplasmic side, but the peptide from Cys187 to Gly188 is running at the extracellular side. The disulfide bond between Cys187 and Cys110 provides support that can make the isomerization efficient. Thus, we suggest that the binding pocket for 11-*cis*-retinal is designed to achieve dual function, holding the retinal as an inverse agonist in the dark, and allowing efficient photoconversion to an agonist.

The methyl group attached to C9 appears to function as a scaffold for these movements to occur efficiently. This interpretation is supported by previous studies, which suggested the important role of this group in the activation of rhodopsin.[16–18] In the ground state, five atoms from Thr118, Ile189, Tyr191, and Tyr268 are located within 4.5 Å from C19. The nonbonded interactions with these residues appear to be critical for stabilizing the 11-*cis* form in the dark and for leading to efficient photoisomerization. In contrast, restraints at this position would be less advantageous for the isomerization of 9-*cis*-rhodopsin, which exhibits similar properties to rhodopsin except for its lower quantum yield.[5]s

Our model of bathorhodopsin also agrees with the previous observation that the β-ionone ring is in the vicinity of Trp265 in both rhodopsin and bathorhodopsin but

approaches Ala169 at TMH-IV in the later intermediates.[9] The curved structure of retinal in bathorhodopsin appears to be consistent with a prediction that it would relax by moving toward TMH-IV (Figure 3d). The initial movement of the β-ionone ring toward the extracellular side prevents a steric clash with TMH-III, mainly at Glu122 (Figure 3c). Then, the distorted all-*trans*-retinal in bathorhodopsin would relax by further movement of the β-ionone ring toward TMH-IV, presumably through a cavity surrounded by Thr118, Glu122, and Cys167 (Figure 3d). Then, the constraints imposed by the retinal on some key residues such as Trp265 and Phe261 in TMH-VI will vanish, allowing the helix freedom to assume the structure of the active state by rigid body movement[19] and/or rotational motion.[20] Photon energy stored in bathorhodopsin would be necessary for these possible dynamic events to occur. Thus, we suggest that the flexible conjugated polyene of retinal is ideal to work as an extremely sensitive photodetector (for more details, see also Reference [13]).

Experimental Section

Microspectrophotometry: Three-dimensional crystals of bovine rhodopsin were grown as reported previously.[2] The changes in the visible absorption spectra of the crystals were recorded by a system based on a 3DX microspectrophotometer with an ANDOR CCD detector. A crystal mounted on the goniometer head was illuminated under a stream of cold (105 K) nitrogen gas by argon laser light, which was depolarized and aligned along the long axis of crystals to maximize the extent of photoreaction. The temperature at the crystal position was recorded by a thermocouple for the goniometer head.

Data collection: All of the X-ray diffraction data sets were collected on a MAR165 CCD detector at BL41XU of SPring-8, with a beam wavelength of 1 Å. The temperature at the position of the crystal was kept at 95 K during data collection. To illuminate the crystals, depolarized argon laser light (488 nm, 2–7 mW) was aligned in a manner similar to that for the offline microspectroscopy experiment and brought to the crystal during data collection. (See Supporting Information for more details.)

Model building and refinement: For the refinement of bathorhodopsin, a model of rhodopsin at 2.2 Å[2] was used as a starting model. Using phases of this structure and after rigid body refinement, F_o-F_o maps were calculated for a number of ground-state (F_{dark}) and illuminated (F_{light}) data sets with different laser light intensities to obtain reproducible structural differences between rhodopsin and bathorhodopsin. We first considered the contribution from the possible 9-*cis* form in the illuminated crystals as described in the Supporting Information. The structure factors were used after appropriate treatment of the twin fractions of the data sets determined by the method described by Yeates.[21] The occupancy of rhodopsin (α) in an illuminated crystal was estimated for each of the data sets by performing alternate conformation refinement of the structure of the intermediate with its occupancy of $1-\alpha$ while the rest (rhodopsin) was fixed. The amino acids included in refinement were Cys110, Glu113, Thr118, Glu122, Cys167, Cys187, Met207, Phe212, Trp265, Tyr268, and Lys296. The value of α was changed from 0.4 to 0.75 in steps of 0.05, and the resulting R_{cryst}, R_{free}, and bonds/angles root-mean-square deviations were compared. Finally, occupancy refinement of the two conformations converged to yield values of $\alpha = 0.65$ with CNS v.1.1.[22] We also carried out the selected-atom structure refinement of the intermediates by using extrapolated structure factor amplitudes $(F_{light}-\alpha F_{dark})/(1-\alpha)$ and found that the

results, including the optimal value of α, were almost the same as those for the alternate conformation refinement.

[1] K. Palczewski, T. Kumasaka, T. Hori, C. A. Behnke, H. Motoshima, B. A. Fox, I. Le Trong, D. C. Teller, T. Okada, R. E. Stenkamp, M. Yamamoto, M. Miyano, *Science* **2000**, *289*, 739–745.

[2] T. Okada, M. Sugihara, A. N. Bondar, M. Elstner, P. Entel, V. Buss, *J. Mol. Biol.* **2004**, *342*, 571–581.

[3] J. Li, P. C. Edwards, M. Burghammer, C. Villa, G. F. X. Schertler, *J. Mol. Biol.* **2004**, *343*, 1409–1438.

[4] R. W. Schoenlein, L. A. Peteanu, R. A. Mathies, C. V. Shank, *Science* **1991**, *254*, 412–415.

[5] J. B. Hurley, T. G. Ebrey, B. Honig, M. Ottolenghi, *Nature* **1977**, *270*, 540–542.

[6] A. Cooper, *Nature* **1979**, *282*, 531–533.

[7] I. Palings, E. M. M. van den Berg, J. Lugtenburg, R. A. Mathies, *Biochemistry* **1989**, *28*, 1498–1507.

[8] E. C. Y. Yan, Z. Ganim, M. A. Kazmi, B. S. W. Chang, T. P. Sakmar, R. A. Mathies, *Biochemistry* **2004**, *43*, 10867–10876.

[9] B. Borhan, M. L. Soutu, H. Imai, Y. Shichida, K. Nakanishi, *Science* **2000**, *288*, 2209–2212.

[10] P. J. R. Spooner, J. M. Sharples, S. C. Goodall, P. H. M. Bovee-Geurts, M. A. Verhoeven, J. Lugtenburg, A. M. A. Pistorius, W. J. DeGrip, A. Watts, *J. Mol. Biol.* **2004**, *343*, 719–730.

[11] S. O. Smith, J. Courtin, H. J. M. de Groot, M. Gebhard, J. Lugtenburg, *Biochemistry* **1991**, *30*, 7409–7415.

[12] Y. Matsui, K. Sakai, M. Murakami, Y. Shiro, S. Adachi, H. Okumura, T. Kouyama, *J. Mol. Biol.* **2002**, *324*, 469–481.

[13] M. Schreiber, M. Sugihara, T. Okada, V. Buss, *Angew. Chem.* **2006**, *118*, 4380–4383; *Angew. Chem. Int. Ed.* **2006**, *45*, 4274–4277.

[14] D. D. Oprian, *J. Bioenerg. Biomembr.* **1992**, *24*, 211–217.

[15] C. D. Strader, M. R. Candelore, W. S. Hill, I. S. Sigal, R. A. F. Dixon, *J. Biol. Chem.* **1989**, *264*, 13572–13578.

[16] U. M. Ganter, E. D. Schmid, D. Perez-Sala, R. R. Rando, F. Siebert, *Biochemistry* **1989**, *28*, 5954–5962.

[17] M. Han, M. Groesbeck, S. O. Smith, T. P. Sakmar, *Biochemistry* **1998**, *37*, 538–545.

[18] C. K. Meyer, M. Bohme, A. Ockenfels, W. Gartner, K. P. Hofmann, O. P. Ernst, *J. Biol. Chem.* **2000**, *275*, 19713–19718.

[19] D. L. Farrens, C. Altenbach, K. Yang, W. L. Hubbell, H. G. Khorana, *Science* **1996**, *274*, 768–770.

[20] L. Shi, G. Liapakis, R. Xu, F. Guarnieri, J. A. Ballesteros, J. A. Javitch, *J. Biol. Chem.* **2002**, *277*, 40989–40996.

[21] T. O. Yeates, *Methods Enzymol.* **1997**, *276*, 344–358.

[22] A. T. Brünger, P. D. Adams, G. M. Clore, W. L. DeLano, P. Gros, R. W. Grosse-Kunstleve, J. S. Jiang, J. Kuszewski, M. Nilges, N. S. Pannu, R. J. Read, L. M. Rice, T. Simonson, G. L. Warren, *Acta. Crystallogr. Sect. D* **1998**, *54*, 905–921.